Afghan International Journal of Science (AIJS)

Publisher: Afghan International Islamic University

Website: https://aijs.aiiu.edu.af

Sensitivity Analysis of Key Mechanical Parameters in the Uniaxial Compressive Strength Test Using Numerical Simulation

***Gholam Ali Rahmani[1], Zaman Nihzat[2], Mohammad Jawad Jahed[3]**

[1]Mining Engineering Department, Mining and Environmental Engineering Faculty, Balkh University, Balkh, AF

[2]Mining Engineering Department, Engineering Faculty, Baghlan University, Baghlan, Afghanistan

[3]Master's Student, Mining Engineering & Management Department, Engineering Faculty, Afghan International Islamic University, Kabul, Afghanistan

Abstract

Predicting the mechanical behavior of rocks under loading is crucial for stability analyses and the design of underground and mining structures. A primary challenge lies in identifying and quantifying the influence of Geomechanical parameters on ultimate strength and failure mechanisms. In this study, a parametric sensitivity analysis was conducted to assess the effects of four key parameters—loading rate, friction angle, cohesion, and Young's modulus—on rock behavior under compressive loading. Numerical simulations were performed by varying each parameter independently while keeping the others constant. Results indicate that increasing the loading rate enhances the peak strength. The ultimate strength is primarily governed by cohesion and the friction angle, whereas Young's modulus affects only stiffness and the slope of the elastic portion of the stress–strain curve, without influencing peak strength. All specimens exhibited post-peak softening, with failure characterized by progressive development of shear zones and fracture surfaces. Cohesion was found to exert a more substantial influence on ultimate strength than the friction angle.

Keywords: Mechanical properties, Numerical modelling, Rock behaviour, Sensitivity analysis, Uniaxial compressive strength.

Article History

Published: Dec 31, 2025

Accepted: Dec 29, 2025

Revised: Dec 29, 2025

Received: Nov 18, 2025

Cite as: Rahmani, G. A., Nihzat, Z., & Jahed, M. J. (2025). Sensitivity Analysis of Key Mechanical Parameters in the Uniaxial Compressive Strength Test Using Numerical Simulation. *Afghan International Journal of Science 1*(1), 89-105. DOI: https://doi.org/10.66546/aijs.v1i1.13

Introduction

The mechanical behaviour of rocks is one of the most fundamental issues in mining engineering. A precise understanding of this behaviour is essential for the design of tunnels, underground spaces, mine foundations, and slope stability analysis (Hoek & Brown, 1997). For this purpose, rock mechanical tests are widely used as primary tools to evaluate and predict the strength and deformability behaviour of rocks under various conditions (Jaeger et al., 2009). Among the key mechanical parameters, the Uniaxial Compressive Strength (UCS) test is crucial. This test serves as a fundamental indicator of intact rock strength and is widely used to

***Correspondence:** gholamali.r75@gmail.com

Link: https://aijs.aiiu.edu.af/index.php/aijs/article/view/13

determine Young's modulus and Poisson's ratio (Bieniawski & Bernede, 1979; Nguyen et al., 2023). Moreover, UCS is broadly applied in rock mass classification, stability analysis, and engineering design (Xie et al., 2025). The mechanical response of rocks under uniaxial compression is governed by parameters such as Young's modulus, Poisson's ratio, cohesion, and friction angle (Rong et al., 2020). However, determining these parameters precisely through laboratory testing can take time and be expensive.

Despite the importance of physical laboratory tests, measuring the UCS under controlled conditions is challenging. The inherent heterogeneity of rock, complex loading conditions, and environmental factors can limit the accuracy and reliability of the obtained results. Consequently, numerical simulation has been widely employed to model rock behaviour under compressive loading (Potyondy & Cundall, 2004). In recent decades, numerical methods have emerged as powerful tools for simulating the complex mechanical behaviour of rocks and analysing Geomechanical problems. Techniques such as the Finite Element Method (FEM), Finite Difference Method (FDM), and Discrete Element Method (DEM) enable accurate modelling of the initiation, propagation, and coalescence of cracks, leading to the final failure of rock specimens (Cundall & Strack, 1979). A key advantage of these numerical approaches is their ability to perform sensitivity analyses, which enable a quantitative assessment of the influence of input parameters on the overall mechanical response.

Over the past two decades, numerous studies have numerically investigated the mechanical behaviour of rocks. Stefanizzi et al. (2009) simulated compression tests on isotropic and homogeneous rock specimens using the FEM-based ELFE2D code. Mahabadi et al. (2014) examined the development of the damaged zone around tunnels in clay-rich rocks using a coupled F-DEM model. Tatone and Grasselli (2015) and Mardalizad et al. (2018) simulated the brittle failure of geomaterials and sandstone through advanced constitutive modelling approaches. Furthermore, Xiong et al. (2021), Xiong et al. (2019), and Kucewicz et al. (2020, 2021) investigated the transition from continuous to discontinuous behaviour of rocks using hybrid FEM–DEM techniques in conjunction with the classical Mohr–Coulomb model. Bahaaddini et al. (2014), Li and Wong (2012), Yang et al. (2014), Zhang and Zhu (2020), and Zhao et al. (2015) also conducted similar studies using LS-DYNA and PFC software to investigate the strength and mechanical behaviour of fractured and cracked rock specimens.

Despite these advancements, most studies have focused primarily on rock failure simulation and model development, while quantitative analyses of the influence of input parameters and their associated uncertainties have received relatively little attention. Incorrect modelling or inaccurate determination of material properties can lead to unreliable predictions of rock behaviour. Therefore, conducting a sensitivity analysis and evaluating the effect of each input parameter are essential to enhance the reliability and robustness of numerical models (Mahabadi et al., 2014), as the model outcomes are highly dependent on these parameters. In fact, Geomechanical parameters of rock are often accepted as constant values, whereas rocks are inherently discontinuous, heterogeneous, anisotropic, and non-elastic (DIANE) materials, characterized by significant uncertainties (Jing & Stephansson, 2007). Moreover, environmental factors such as weathering, water saturation, and thermal cycling can degrade

rock strength and influence the stability of engineering structures (Lee et al., 2021). Additionally, the loading rate can alter the rock behaviour from a semi-static to a dynamic regime (Chang et al., 2006).

Therefore, a quantitative and systematic understanding of the influence of input parameters on the compressive strength and failure mechanisms of rocks is essential. The present study aims to address this gap by performing a numerical sensitivity analysis of the UCS test on an iron ore rock sample. In this research, a numerical model was developed using the FDM and calibrated using laboratory test data. Subsequently, the effects of varying parameters—including loading rate, internal friction angle, cohesion, and Young's modulus—on the ultimate rock strength and failure pattern were comprehensively investigated. The findings of this study contribute to a deeper understanding of rock behaviour, providing valuable insights for risk assessment and the optimization of engineering design and stability analysis in Geomechanical applications.

Methods and Materials

Laboratory Uniaxial Compressive Strength Test

The uniaxial compressive strength test was performed in accordance with the guidelines of the International Society for Rock Mechanics (ISRM) (Bieniawski & Bernede, 1979). Cylindrical iron ore specimens with a diameter of 51 mm and a length of 127 mm were prepared from intact rock material. Before testing, the ends of each specimen were meticulously ground and levelled to ensure uniform load distribution during axial compression. The samples were then subjected to uniaxial loading until failure.

During testing, both the applied axial load and the corresponding deformation were continuously monitored and recorded. Upon completion of the experiment, the rock's mechanical parameters were determined. To obtain the cohesion and internal friction angle of the iron ore, additional specimens of the same lithology were tested under triaxial compression. The mechanical and strength characteristics of the iron ore samples are presented in Table 1.

Table 1: *Mechanical and Strength Properties of the Iron Ore specimen*

No	Parameters	Value	Unit
1	Uniaxial Compressive Strength	44.5	MPa
2	Density	3810	Kg/m^3
3	Young's Modulus	14	GPa
4	Poisson's Ratio	0.45	-
5	Internal Friction angle	37.9	Degree
6	Cohesion	12	MPa

To further investigate the mechanical behaviour of the specimen, the stress–strain curve obtained from the uniaxial compression test was plotted in Figure 1 below. This curve clearly illustrates the elastic region and the peak strength point, which are in good agreement with the values presented in Table 1.

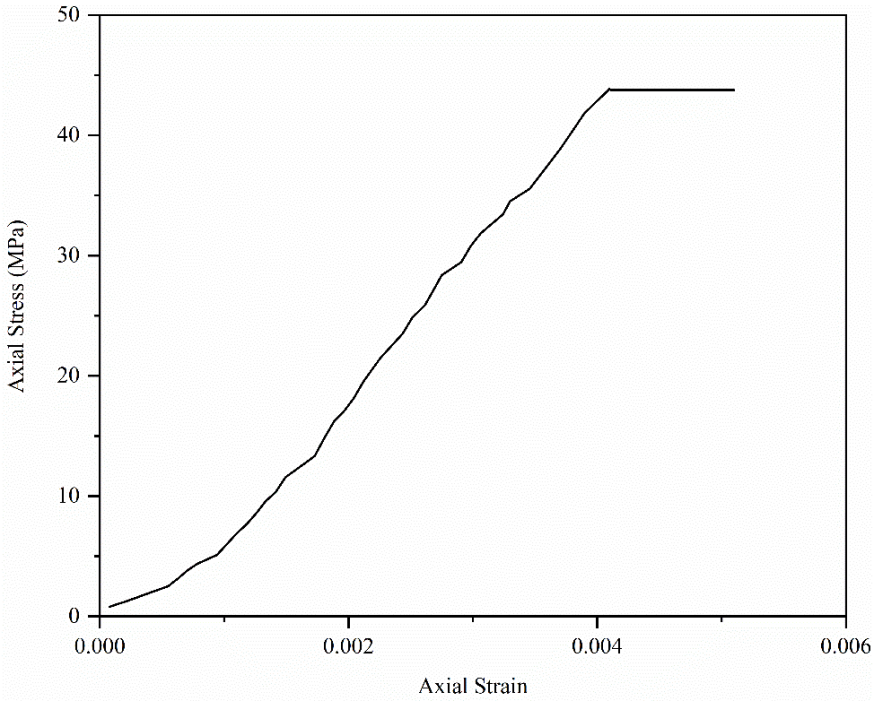

Figure 1: *Stress-Strain curve of Uniaxial Compression Test*

Numerical Modelling

In this study, the finite difference method was used to simulate the UCS test in FLAC2D. The numerical model was developed based on the actual geometry of the laboratory specimen, as shown in Figure 2.

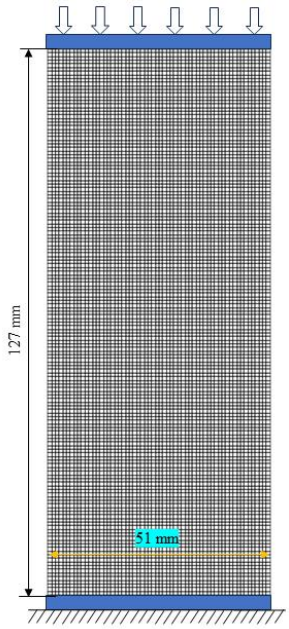

Figure 2: *Geometric Model of the Specimen*

A cylindrical sample with a height-to-diameter ratio of 2:1 was employed for the uniaxial compression simulation. FLAC2D was chosen for its robust capability to model nonlinear material behaviour and capture complex failure mechanisms, making it an appropriate tool for

analysing uniaxial compressive strength (Itasca, 2016). In the numerical model, the bottom of the specimen was fully fixed perpendicular to the base, while a uniform downward velocity was applied to the top surface to induce compressive loading. Throughout the simulation, key data, including the stress–strain curve and the failure mechanisms, were extracted and analysed.

Mechanical Parameters and Constitutive Model

The mechanical input parameters used in the numerical modelling were derived from the laboratory test results summarized in Table 1. In the simulations, the specimen was represented as a homogeneous, isotropic, and elastoplastic material. To characterize the rock's mechanical response, the Mohr–Coulomb constitutive model incorporating strain-softening behavior under axisymmetric conditions was adopted.

Findings

Model Validation

In the numerical simulation, the mechanical parameters of the selected models were calibrated to achieve results consistent with the experimental data. To validate the numerical model, the numerically obtained stress–strain curve was compared with the experimental stress–strain curve. Initially, the mechanical input parameters in the simulation yielded higher compressive strengths than those observed experimentally. To improve the agreement, the values of Young's modulus, Poisson's ratio, and cohesion were gradually reduced. After this calibration process, the numerical stress–strain curve showed good agreement with the experimental curve. As illustrated in Figure 3, although slight discrepancies were observed during the initial loading phase, a satisfactory match was achieved in the peak-strength region. However, certain modelling assumptions—such as the homogeneous representation of the rock, the neglect of micro-discontinuities, and the exclusion of moisture effects—represent the main limitations of the present numerical analysis. The numerical and experimental stress–strain curves are presented in Figure 3.

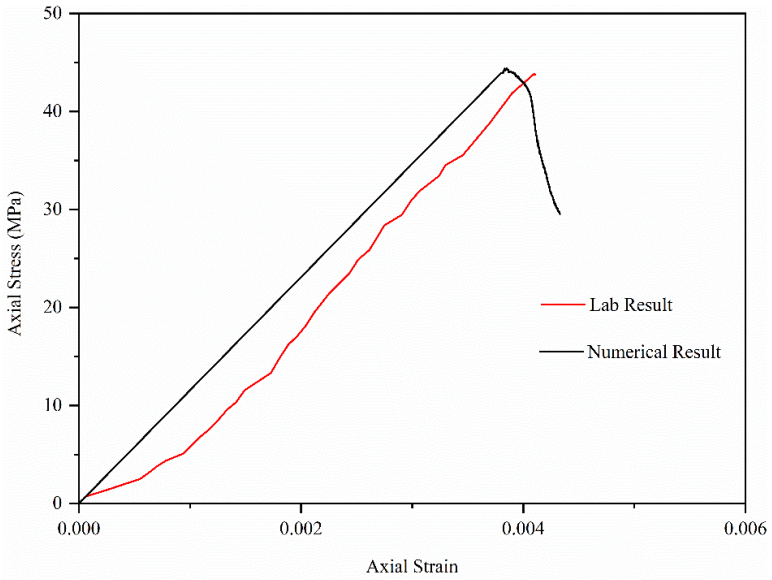

Figure -3 *Stress–strain curves from experimental and numerical analyses*

After calibrating the numerical model, the rock's mechanical parameters were adjusted to match the experimental data. Table 2 presents the final mechanical parameters used in the numerical model. As shown, the values of Young's modulus, Poisson's ratio, and cohesion were reduced to align the numerical stress–strain behaviour with the experimental curve, while density and internal friction angle remained unchanged. This consistency confirms the numerical model's validity in accurately reproducing the rock's mechanical behaviour.

Table 2: *Geomechanical Parameters after Calibration*

No.	Parameters	Value	Unit
1	Uniaxial Compressive Strength	44.5	MPa
2	Density	3810	Kg/m^3
3	Young's Modulus	11.5	GPa
4	Poisson's Ratio	0.34	-
5	Internal Friction angle	37.9	Degree
6	Cohesion	10.7	MPa

Effect of Loading Rate

To achieve a more precise understanding of the specimen behaviour in the UCS test, the effect of loading rate was investigated. For this purpose, four loading rates of 5×10^{-10}, 1×10^{-9}, 5×10^{-9}, and 1×10^{-8} m/s were considered, and the resulting stress–strain curves were compared with the experimental results. The corresponding loading curves are shown in Figure 4.

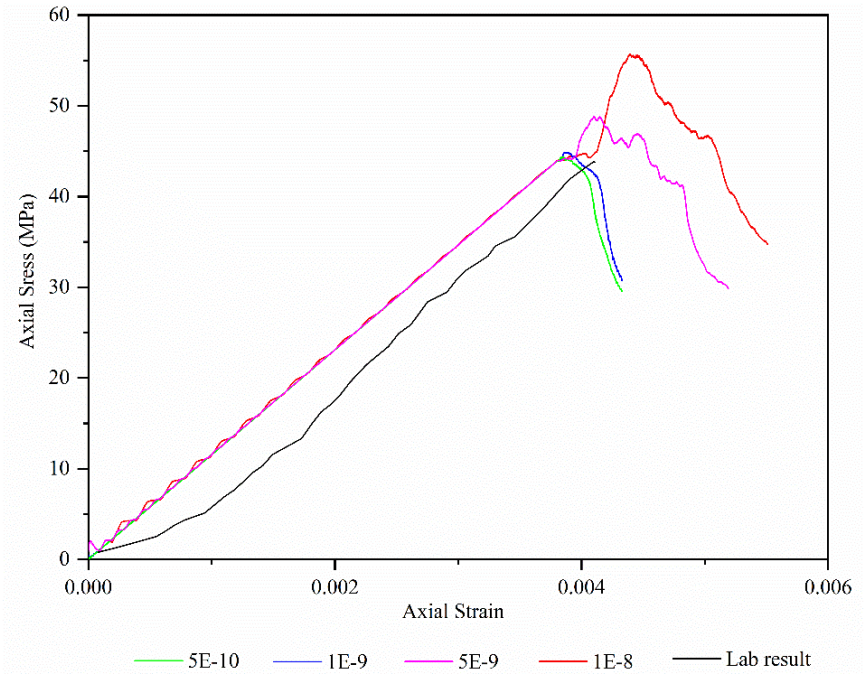

Figure -4 Numerical stress–strain curves at different loading rates compared with the experimental curve

In the elastic phase of the curve, no significant difference was observed between the numerical and experimental results, indicating that the loading rate has only a minor effect on the initial stiffness or Young's modulus. However, as the stress approached the peak strength, noticeable differences began to appear. Higher loading rates increased peak strength and altered the post-failure behaviour of the specimens. The results demonstrate that the loading rate plays a crucial

role in the rock sample's actual behaviour. As shown in Figure 4, decreasing the loading rate resulted in closer agreement between the numerical and experimental stress–strain curves. This finding indicates that when loading is applied gradually at a lower rate, the stress distribution becomes more uniform, and the numerical response better reflects the material's real mechanical behaviour.

Although reducing the loading rate yields more accurate results, it significantly increases the computation time and makes the model execution more demanding. Based on this study's findings, a loading rate below 1×10^{-9} m/s is considered optimal, as it ensures both accurate results and acceptable computational efficiency. In general, the selection of the loading rate in numerical analyses should be based on a balance between result accuracy and computational cost. This outcome can serve as a practical guideline for similar numerical studies and highlights the importance of properly managing loading rate in mechanical rock simulations.

Parametric Sensitivity Analysis

In this section, a sensitivity analysis was performed to investigate the influence of key parameters on the model's response. In this stage, each parameter was varied individually within a defined range, while the others were kept constant. The analysis focused on three fundamental parameters: internal friction angle (ϕ), cohesion (c), and Young's modulus (E), to examine their effects on the UCS behaviour. This approach provides a deeper understanding of the mechanisms governing the rock model's mechanical response. The following subsections present the influence of each parameter separately.

Effect of Friction Angle

The internal friction angle is one of the primary parameters in shear failure criteria, such as the Mohr–Coulomb model, and it defines the material's resistance to sliding along internal planes. To evaluate the influence of this parameter, UCS were simulated with friction angles ranging from 33° to 37.9°, while keeping all other parameters constant. The results of these simulations are presented as axial stress–strain curves in Figure 5.

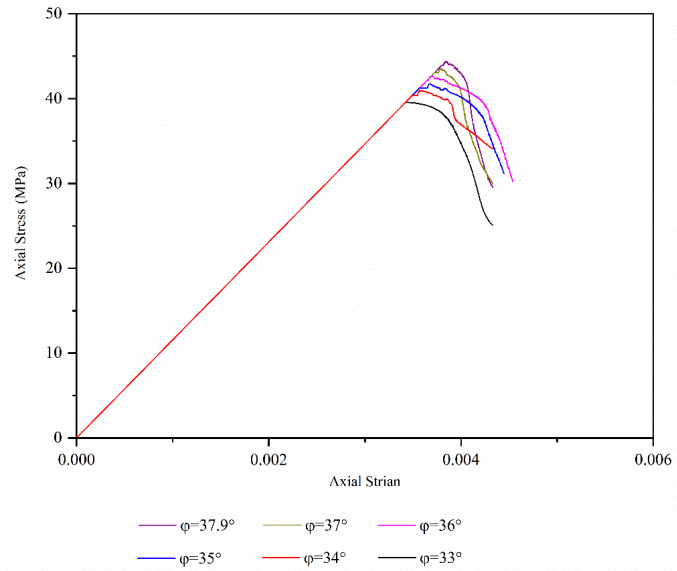

Figure -5 Axial stress–strain curves from numerical simulations with different internal friction angles

As shown in the figure, all curves exhibit similar behaviour: an initial linear-elastic region, a plastic deformation stage, and a peak strength. Beyond this point, the specimens exhibit strain-softening behaviour, characterized by a gradual reduction in strength after failure initiation.

The results clearly indicate a direct relationship between the internal friction angle and the uniaxial compressive strength. With a decrease in the friction angle from 37.9° to 33°, the peak strength value decreases significantly. This is also physically expected, since a larger internal friction angle implies greater interparticle interlocking and greater resistance to shear failure. In fact, this parameter directly affects and widens the material's failure envelope. The initial slope of all curves in the elastic region completely overlaps, confirming that the internal friction angle does not influence the elastic stiffness of the rock. Young's modulus is an intrinsic parameter related to the material's elastic behaviour, whereas the internal friction angle governs its plastic behaviour and failure. However, the general post-failure pattern across all models shows that strain softening, the onset of yielding, and the entry into the plastic region shift with changes in ϕ. Models with higher friction angles can sustain larger plastic strains before reaching the peak point and enter the softening region at higher stress levels. Figure 6 illustrates the failure mechanisms of samples for different values of the internal friction angle. The results consistently show a shear failure mechanism initiating from the upper corner of the specimen and propagating inward. Comparative analysis of the samples reveals that as the friction angle decreases from 37.9° to 33°, although the overall failure pattern remains similar, the damaged zone becomes significantly broader and more dispersed. At higher values of ϕ, failure is concentrated along a narrow shear band, indicating brittle behaviour in the samples, whereas at lower values, the damage is distributed over a larger volume of the specimen, reflecting a reduction in the degree of brittleness of the rock.

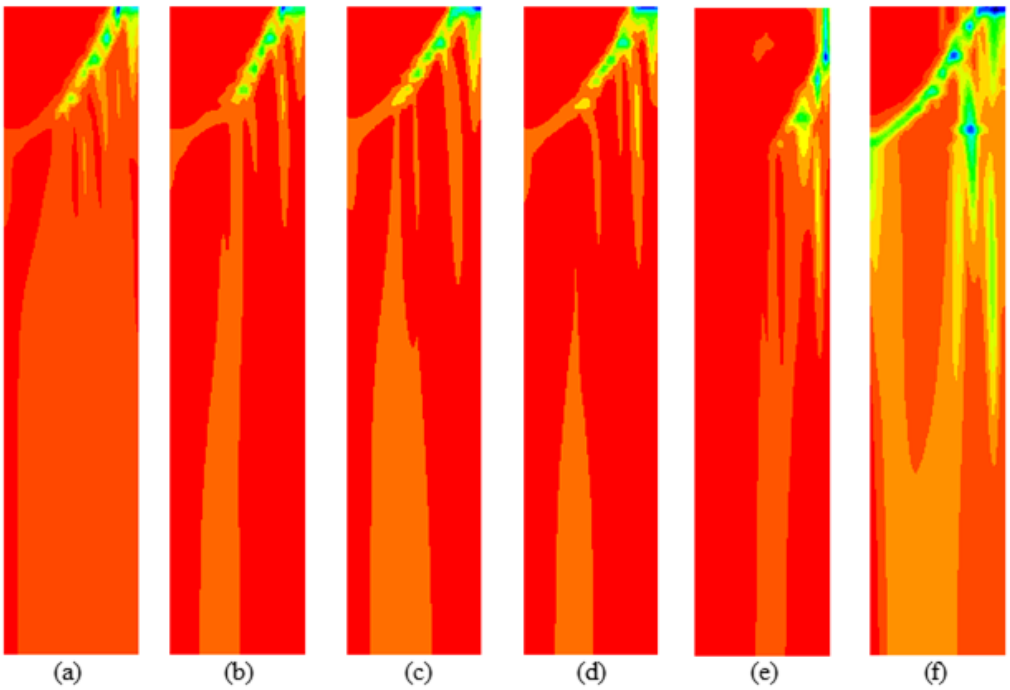

Figure 6: *Plastic shear strain contours illustrate the failure mechanism of the specimen in the UCS test for different values of internal friction angle: (a) 37.9°, (b) 37°, (c) 36°, (d) 35°, (e) 34°, and (f) 33°.*

The initiation of failure from the corners of the specimen is likely due to stress concentration at the points of contact between the specimen and the loading plates, or to end effects resulting from friction between the specimen and the plates. This friction induces a localized confinement at both ends of the specimen, increasing the strength of those regions. Consequently, failure tends to initiate from zones of high stress concentration located outside these strengthened areas — namely, from the specimen corners.

Effect of Cohesion

Cohesion plays a fundamental role in the shear strength, stability, and load-bearing capacity of intact rock. This parameter represents the material's intrinsic resistance to sliding. To quantify the influence of cohesion on the mechanical behaviour of the model, a series of uniaxial compression simulations was conducted with varying cohesion values ranging from 6 to 10.7 MPa. In this analysis, all other input parameters were kept constant. The obtained results are illustrated in Figure 7.

The results clearly demonstrate a linear and direct relationship between cohesion and uniaxial compressive strength. As cohesion decreases from 10.7 MPa to 6 MPa, the peak strength of the specimen drops from approximately 44.5 MPa to 25 MPa. Similar to the analysis of the internal friction angle, it is observed here that the initial slopes of all curves in the elastic region are identical. This complete overlap indicates that cohesion, as a strength parameter, does not affect the material's elastic stiffness or Young's modulus. Another noteworthy point is that, as cohesion increases, the axial strain at peak strength also increases. In other words, materials with higher cohesion are not only stronger but can also undergo greater plastic deformation before complete failure, indicating a slight increase in ductility prior to reaching the peak point.

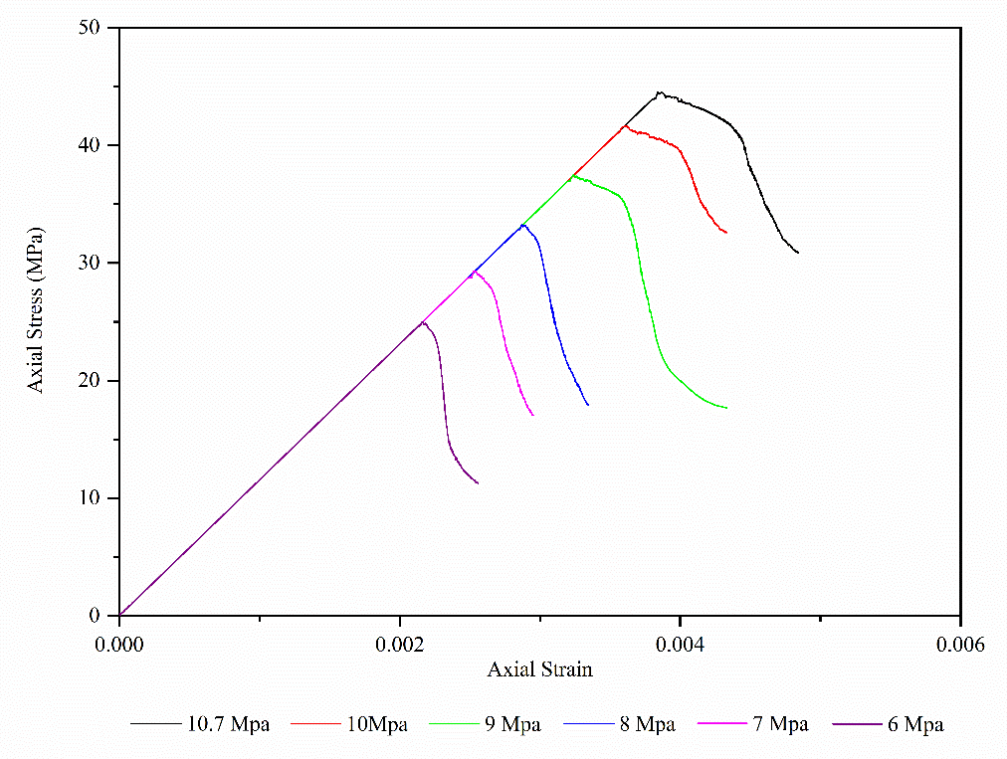

Figure 7: *Stress–strain curves obtained from numerical simulations for different cohesion values*

The plastic shear strain contours presented in Figure 8 illustrate the failure mechanisms of specimens in uniaxial compression tests for different cohesion values. As shown, when cohesion decreases from 10.7 MPa to 6 MPa, both the intensity of strain concentration and the failure pattern change, resulting in broader, deeper failure zones within the specimen. At higher cohesion values (Figures a and b), failure is mainly localized near the loading surfaces, and the failure paths remain limited.

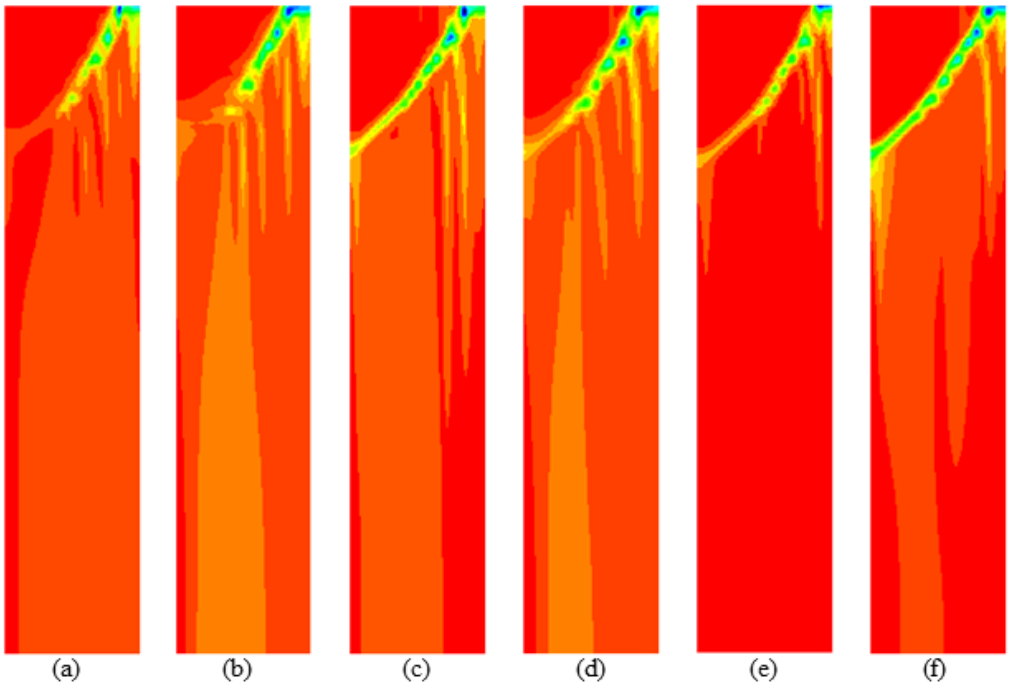

Figure -8 Plastic shear strain contours illustrating the failure mechanism of the specimen in the UCS test for different cohesion values: (a) 10.7 MPa, (b) 10 MPa, (c) 9 MPa, (d) 8 MPa, (e) 7 MPa, and (f) 6 MPa.

With the gradual reduction in cohesion (Figures c-f), the failure paths evolve into a combined shear–tensile pattern and penetrate deeper into the specimen. This indicates that decreasing cohesive strength leads to the dominance of more extensive shear mechanisms and, ultimately, a reduction in the specimen's load-bearing capacity. Therefore, variations in cohesion play a key role in determining the type and extent of failure propagation and directly influence the mechanical behaviour of the specimen under uniaxial compressive loading.

Effect of Young's modulus

Young's modulus, as a measure of material stiffness, characterizes the rock's deformation behavior within the elastic range. To assess the model's sensitivity to this parameter, a series of numerical simulations was conducted using Young's modulus values ranging from 7 to 11.5 GPa, while keeping all other parameters constant. The results of this analysis are illustrated in Figure 9.

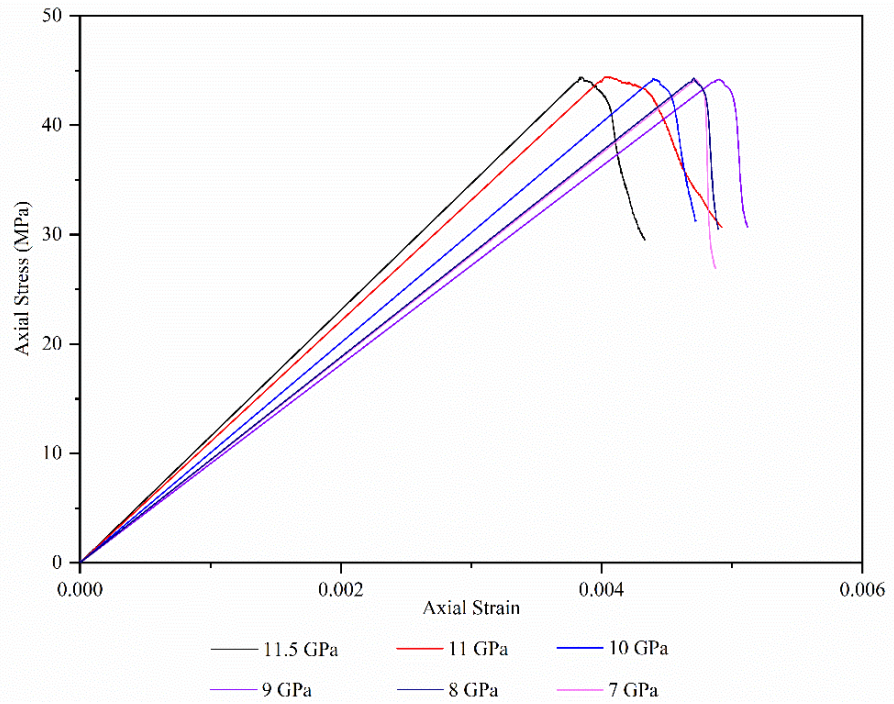

Figure 9: *Axial stress–strain curves obtained from numerical simulations for different values of Young's modulus*

The most evident effect of Young's modulus is observed in the slope of the linear elastic portion of the stress–strain graphs. As expected, there is a direct relationship between the value of E and the slope of the curve. The model with the highest Young's modulus (E = 11.5 GPa) exhibits the steepest slope, indicating the highest material stiffness. As E decreases, the curves' slopes decrease systematically, and at the lowest value (E = 7 GPa), the slope is the gentlest. This clearly demonstrates that Young's modulus governs the model's deformation behaviour prior to yielding. The results confirm that Young's modulus, as an elastic parameter, has a negligible effect on the material's ultimate UCS. As shown in Figure 9, all curves reach their peak strength at nearly the same level (approximately 44 MPa). This finding is significant because it indicates that the material strength in this model is accurately controlled by the failure criterion parameters (cohesion and internal friction angle), whereas the elastic stiffness does not determine the failure level.

On the other hand, the strain corresponding to the peak stress shifts with changes in Young's modulus. Softer materials with lower E values require greater strain and deformation to reach their ultimate load-bearing capacity. This trend is clearly visible in the curves: the peak point shifts from an approximate strain of 0.0039 for E = 11.5 GPa to about 0.0050 for E = 7 GPa. The plastic shear strain contours shown in Figure 10 illustrate how the failure mechanism of the specimen under uniaxial compression varies with different Young's modulus values. As E decreases from 11.5 GPa (Figure 10a) to 7 GPa (Figure 10f), the distribution of shear strain changes, with the failure zones becoming broader and more profound. At higher Young's modulus values, stress concentration and failure remain localized and limited, indicating higher stiffness and brittleness of the material.

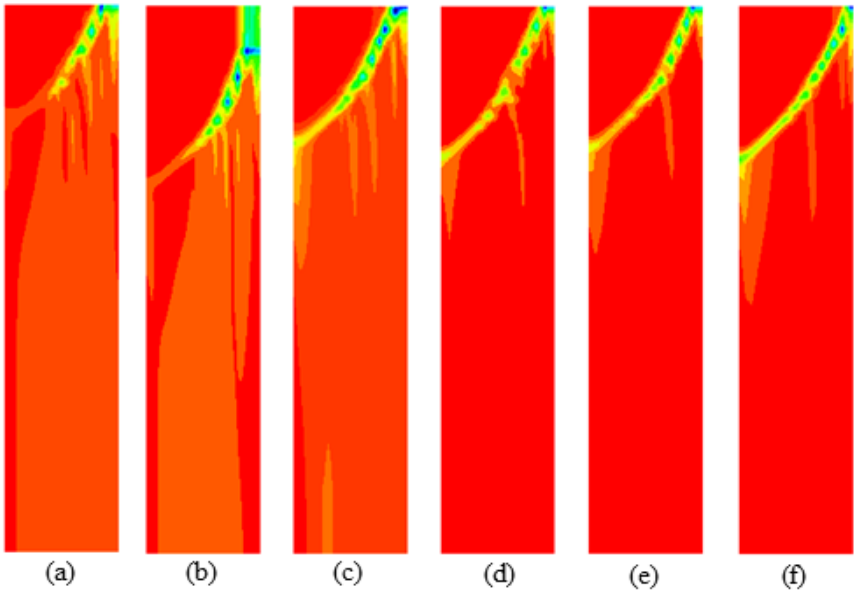

Figure -10 Plastic shear strain contours illustrating the failure mechanism of the specimen in the uniaxial compression test for different values of Young's modulus: (a) 11.5 GPa, (b) 11 GPa, (c) 10 GPa, (d) 9 GPa, (e) 8 GPa, and (f) 7 GPa.

However, with the decrease in Young's modulus, the specimen becomes more ductile, and failure—rather than being concentrated in a specific region—spreads diffusely and continuously along the loading surface and within the specimen. This change indicates that the reduction in elastic stiffness leads to increased plastic deformation and the development of more extensive failure paths. Therefore, Young's modulus plays a decisive role in controlling the mechanical behaviour and failure pattern of the specimens, directly influencing both the load-bearing capacity and the formation of discontinuities. Figure 11 illustrates the effect of variations in cohesion and internal friction angle on UCS. As observed, both parameters exhibit a direct and positive correlation with the ultimate strength of the specimen. Graph (a) shows that as cohesion increases from 6 MPa to 11 MPa, the UCS rises from 25 MPa to approximately 45 MPa. Similarly, Graph (b) indicates that increasing the internal friction angle from 33° to 38° raises the uniaxial compressive strength from about 39.5 MPa to 44.5 MPa.

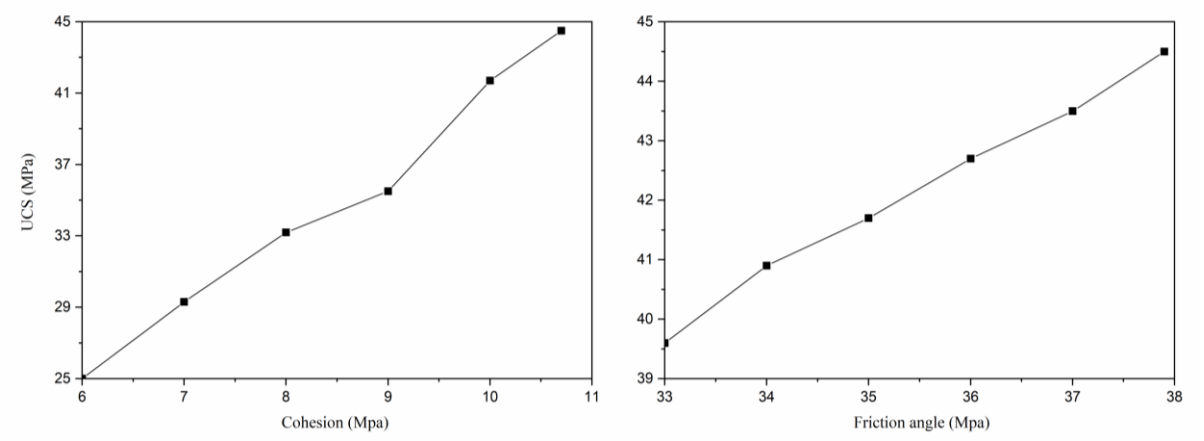

Figure 11: *Comparison of the effects of cohesion and internal friction angle on uniaxial compressive strength*

A comparison of the two graphs reveals a significant difference in the degree of sensitivity of UCS to each parameter. The slope of the cohesion variation curve is considerably steeper than that of the internal friction angle curve. More specifically, the numerical results indicate that for every 1 MPa increase in cohesion, the ultimate strength of the specimen increases by approximately 4 MPa, whereas a 1° increase in the internal friction angle results in only about a 1 MPa increase in ultimate strength.

This finding indicates that, within the range of parameters examined for this type of rock, cohesion is the dominant parameter controlling uniaxial compressive strength, rather than the internal friction angle. This has important implications for stability analysis and design, as it demonstrates that uncertainty in cohesion measurements can lead to much larger errors in estimating rock strength.

Discussion

The parametric sensitivity analysis conducted in this study was not only a necessary step for validating the numerical model but also an effective means of distinguishing between the parameters governing rock strength and deformability. The results indicate that the developed numerical model exhibits realistic physical behaviour. The strong dependence of UCS on the parameters of cohesion (c) and internal friction angle (ϕ) is entirely consistent with the framework of conventional rock mechanics failure criteria—particularly the Mohr–Coulomb failure criterion. This criterion, which underlies many stability analyses, defines shear strength as a linear function of normal stress, with c and ϕ representing the intercept and slope of the failure envelope, respectively (Brady & Brown, 2006). Our results clearly demonstrated that reducing either parameter reduces the overall model strength, confirming that the failure behaviour is governed by both frictional and cohesive mechanisms within the rock structure. This finding underscores the critical importance of accurately determining these two parameters in laboratory studies, since—as noted by many researchers—uncertainty in c or ϕ can directly lead to significant uncertainty in predicting the stability of rock structures such as tunnels and slopes (Hoek & Diederichs, 2006).

In contrast, the results of the Young's modulus sensitivity analysis showed that although this parameter primarily controls stiffness and pre-failure deformation behaviour, it has only a limited influence on the ultimate strength. This separation of roles is one of the fundamental characteristics of elastoplastic constitutive models, in which elastic behaviour is defined by (E, ν), while plastic behaviour is controlled by (c, ϕ)—a set of independent parameters(Potts et al., 2001). This observation is critical from an engineering perspective: it underscores that, for analyses in which deformation and displacement are the primary design criteria, the accurate determination of Young's modulus is essential. However, in ultimate limit-state analyses focusing on failure and collapse, the strength parameters (c and ϕ) play a dominant role.

Conclusion

In this study, four key parameters—internal friction angle, cohesion, Young's modulus, and loading rate—were investigated to assess their influence on the mechanical behaviour of rock specimens under uniaxial compressive loading. The results reveal that these parameters exert

different effects on the mechanical response of the specimens. Ultimate strength is directly controlled by the internal friction angle, cohesion, and loading rate, so that an increase in any of these parameters leads to a significant increase in peak strength. Analysis of the stress–strain curves showed that all models, after reaching their peak strength, entered a strain-softening stage, exhibiting a gradual decrease in stress. The corresponding failure mechanism involved the progressive development of shear zones and the formation of a distinct failure plane within the model. This trend indicates that, while the ultimate strength depends on the strength parameters, the post-peak failure pattern is also governed by the degree of interlocking between particles and the internal bonding within the rock.

In contrast, Young's modulus only affected the distribution and magnitude of strain before the peak, without decisively influencing the final failure mechanism. Furthermore, the comparison between the internal friction angle and cohesion showed that cohesion has a more substantial influence on the ultimate strength of the rock specimen. For future work, it is recommended that digital imaging and microscopic analysis techniques be used in conjunction with numerical modelling to evaluate microcrack development and the evolution of failure surfaces in greater detail. Additionally, extending the parametric sensitivity analysis using alternative failure criteria is suggested to validate the robustness of the findings further further.

Authors Contributions

- Gholam Ali Rahmani investigated and analyzed data and performed the numerical modelling.
- Zaman Nihzat and Mohammad Jawad Jahed wrote the manuscript with input from all authors.
- All authors reviewed and approved the final version.

References

Bahaaddini, M., Hagan, P. C., Mitra, R., & Hebblewhite, B. K. (2014). Scale effect on the shear behaviour of rock joints based on a numerical study. *Engineering Geology*, *181*, 212-223. https://doi.org/10.1016/j.enggeo.2014.07.018

Bieniawski, Z. T., & Bernede, M. J. (1979). Suggested methods for determining the uniaxial compressive strength and deformability of rock materials: Part 1. Suggested method for determining the deformability of rock materials in uniaxial compression. *International Journal of Rock Mechanics and Mining Sciences & Geomechanics Abstracts*, *16*(2), 138-140. https://doi.org/10.1016/0148-9062(79)91451-7

Brady, B. H., & Brown, E. T. (2006). *Rock mechanics: for underground mining*. Springer science & business media. https://doi.org/10.1007/978-1-4020-2116-9

Chang, C., Zoback, M. D., & Khaksar, A. (2006). Empirical relations between rock strength and physical properties in sedimentary rocks. *Journal of Petroleum Science and Engineering*, *51*(3), 223-237. https://doi.org/10.1016/j.petrol.2006.01.003

Cundall, P. A., & Strack, O. D. L. (1979). A discrete numerical model for granular assemblies. *Geotechnique*, *29*(1), 47-65. https://doi.org/10.1680/geot.1979.29.1.47

Hoek, E., & Brown, E. T. (1997). Practical estimates of rock mass strength. *International Journal of Rock Mechanics and Mining Sciences*, *34*(8), 1165-1186. https://doi.org/10.1016/S1365-1609(97)80069-X

Hoek, E., & Diederichs, M. S. (2006). Empirical estimation of rock mass modulus. *International Journal of Rock Mechanics and Mining Sciences*, *43*(2), 203-215. https://doi.org/10.1016/j.ijrmms.2005.06.005

Itasca Consulting Group. (2016). *FLAC: Fast Lagrangian Analysis of Continua (Version 8.0) [Computer software]*. Itasca Consulting Group.

Jaeger, J. C., Cook, N. G., & Zimmerman, R. (2009). *Fundamentals of rock mechanics*. John Wiley & Sons. https://doi.org/10.1017/CBO9780511735349

Jing, L., & Stephansson, O. (2007). *Fundamentals of discrete element methods for rock engineering: theory and applications*. Elsevier. https://doi.org/10.1016/j.ijrmms.2008.04.003

Kucewicz, M., Baranowski, P., & Małachowski, J. (2020). Determination and validation of Karagozian-Case Concrete constitutive model parameters for numerical modeling of dolomite rock. *International Journal of Rock Mechanics and Mining Sciences*, *129*, 104302. https://doi.org/10.1016/j.ijrmms.2020.104302

Kucewicz, M., Baranowski, P., & Małachowski, J. (2021). Dolomite fracture modeling using the Johnson-Holmquist concrete material model: Parameter determination and validation. *Journal of Rock Mechanics and Geotechnical Engineering*, *13*(2), 335-350. https://doi.org/10.1016/j.jrmge.2020.09.007

Lee, S.-H., Chung, C.-K., Song, Y.-W., & Woo, S.-I. (2021). Relationship between Chemical Weathering Indices and Shear Strength of Highly and Completely Weathered Granite in South Korea. *Applied Sciences*, *11*(3), 911. https://doi.org/10.3390/app11030911

Li, H., & Wong, L. N. Y. (2012). Influence of flaw inclination angle and loading condition on crack initiation and propagation. *International Journal of Solids and Structures*, *49*(18), 2482-2499. https://doi.org/10.1016/j.ijsolstr.2012.05.012

Mahabadi, O., Kaifosh, P., Marschall, P., & Vietor, T. (2014). Three-dimensional FDEM numerical simulation of failure processes observed in Opalinus Clay laboratory samples. *Journal of Rock Mechanics and Geotechnical Engineering*, *6*(6), 591-606. https://doi.org/10.1016/j.jrmge.2014.10.005

Mardalizad, A., Scazzosi, R., Manes, A., & Giglio, M. (2018). Testing and numerical simulation of a medium strength rock material under unconfined compression loading. *Journal of Rock Mechanics and Geotechnical Engineering*, *10*(2), 197-211. https://doi.org/10.1016/j.jrmge.2017.11.009

Nguyen, P. M. V., Walentek, A., Waclawik, P., Soucek, K., & Antoniuk, M. (2023). Numerical modelling of Uniaxial Compressive Strength laboratory tests. *Journal of Sustainable Mining*, *22*(4), 280-294. https://doi.org/10.46873/2300-3960.1393

Potts, D. M., Zdravković, L., Addenbrooke, T. I., Higgins, K. G., & Kovačević, N. (2001). *Finite element analysis in geotechnical engineering: application* (Vol. 2). Thomas Telford London. https://doi.org/10.1680/feaigea.27831

Potyondy, D. O., & Cundall, P. A. (2004). A bonded-particle model for rock. *International Journal of Rock Mechanics and Mining Sciences*, *41*(8), 1329-1364. https://doi.org/10.1016/j.ijrmms.2004.09.011

Rong, H., Li, G., Liang, D., Sun, C., Zhang, S., & Sun, Y. (2020). Numerical Investigation on the Evolution of Mechanical Properties of Rock Affected by Micro-Parameters. *Applied Sciences*, *10*(14), 4957. https://www.mdpi.com/2076-3417/10/14/4957

Stefanizzi, S., Barla, G., Kaiser, P., & Grasselli, G. (2009). Numerical modeling of standard rock mechanics laboratory tests using a finite/discrete element approach. Proceedings of the 3rd CANUS Rock Mechanics Symposium, Toronto, canada

Tatone, B. S., & Grasselli, G. (2015). A calibration procedure for two-dimensional laboratory-scale hybrid finite–discrete element simulations. *International Journal of Rock Mechanics and Mining Sciences*, *75*, 56-72. https://doi.org/10.1016/j.ijrmms.2015.01.011

Xie, W.-Q., Liu, X.-L., Zhang, X.-P., Liu, Q.-S., & Wang, E.-Z. (2025). A review of test methods for uniaxial compressive strength of rocks: Theory, apparatus and data processing. *Journal of Rock Mechanics and Geotechnical Engineering*, *17*(3), 1889-1905. https://doi.org/10.1016/j.jrmge.2024.05.003

Xiong, L., Chen, H., & Geng, D. (2021). Uniaxial compression study on mechanical properties of artificial rock specimens with cross-flaws. *Geotechnical and Geological Engineering*, *39*, 1667-1681. https://doi.org/10.1007/s10706-020-01584-z

Xiong, L., Yuan, H., Zhang, Y., Zhang, K., & Li, J. (2019). Experimental and numerical study of the uniaxial compressive stress-strain relationship of a rock mass with two parallel joints. *Archives of Civil Engineering*, 67-80-67-80. https://doi.org/10.2478/ace-2019-0019

Yang, S.-Q., Huang, Y.-H., Jing, H.-W., & Liu, X.-R. (2014). Discrete element modeling on fracture coalescence behavior of red sandstone containing two unparallel fissures under uniaxial compression. *Engineering Geology*, *178*, 28-48. https://doi.org/10.1016/j.enggeo.2014.06.005

Zhang, L., & Zhu, J. (2020). Analysis of mechanical strength and failure morphology of prefabricated closed cracked rock mass under uniaxial compression. *Geotechnical and Geological Engineering*, *38*, 4905-4915. https://doi.org/10.1007/s10706-020-01335-0

Zhao, W., Huang, R., & Yan, M. (2015). Mechanical and fracture behavior of rock mass with parallel concentrated joints with different dip angle and number based on PFC simulation. *Geomech. Eng*, *8*(6), 757-767. https://doi.org/10.12989/gae.2015.8.6.757